Nanoscale Res Lett (2010) 5:1424–1430
DOI 10.1007/s11671-010-9656-4

NANO EXPRESS

Quantum Capacitance Extraction for Carbon Nanotube Interconnects

Vidur Parkash · Ashok K. Goel

Received: 2 March 2010 / Accepted: 19 May 2010 / Published online: 8 June 2010

Abstract Electrical transport in metallic carbon nanotubes, especially the ones with diameters of the order of a few nanometers can be best described using the Tomanaga Luttinger liquid (TL) model. Recently, the TL model has been used to create a convenient transmission line like phenomenological model for carbon nanotubes. In this paper, we have characterized metallic nanotubes based on that model, quantifying the quantum capacitances of individual metallic single walled carbon nanotubes and crystalline bundles of single walled tubes of different diameters. Our calculations show that the quantum capacitances for both individual tubes and the bundles show a weak dependence on the diameters of their constituent tubes. The nanotube bundles exhibit a significantly large quantum capacitance due to enhancement of density of states at the Fermi level.

Introduction

Recently carbon nanotubes have acquired importance as a material with a wide variety of potential applications in nanoelectronics. A significant amount of interest has been generated in metallic carbon nanotubes for their application as an on-chip interconnect, replacing the traditional copper wires which are nearing their performance limits. The International Technology Roadmap for Semiconductors (ITRS) has already placed carbon nanotubes as a potential candidate interconnect material for technology nodes beyond 22 nm [1]. The propagation speed of a signal on a transmission line is related to distributed inductance and capacitance of the system as $v = 1/\sqrt{LC}$. For mesoscopic systems, the capacitance term C comprises a second "quantum" component apart from the Maxwellian capacitance. This parameter is related to the electronic structure of the material. In this paper, we present calculations that illustrate how the quantum capacitance of different carbon nanotubes vary with size and chirality. This information is necessary to construct a simulation model that will be able to characterize nanotube performance accurately.

It has been long known that the Fermi liquid model is not able to describe transport properties of one dimensional metals. The presence of strong electron–electron interactions prevents the formation of a sharp Fermi surface as would be conventionally expected in a regular bulk metal. The Tomanaga Luttinger (TL) model is used to describe electronic transport in one dimensional systems such as a 1D electron gas as present in a carbon nanotube. The TL model attempts to describe transport properties of a 1D electron gas taking into account strong electron–electron correlation, for energies in the vicinity of the Fermi level. The model is constructed by linearizing the energy-wave-vector dispersion of the nanotube around the Fermi wave vector and mapping it onto an equivalent system of boson quasiparticles [2]. Recently, the use of the concepts of Luttinger liquid theory was suggested by authors in [3, 4] to build a phenomenological model of microwave transport in these nanotubes. The authors created a transmission line model mapping a Luttinger model-based Lagrangian to a conventional LC lossless transmission line model. This model is used as a starting point in this paper and has four principal components. These are the classical Maxwellian capacitance (C_{es}) and inductance (L_m), a quantum component of capacitance (C_q) and a kinetic inductance term (L_k). The quantum capacitance is a manifestation of finite size

V. Parkash (✉) · A. K. Goel
Department of Electrical and Computer Engineering, Michigan Technological University, Houghton, MI 49931, USA
e-mail: vparkash@mtu.edu

quantization effects in nanotubes. The electrostatic capacitance C_{es} is related to the electron–electron interactions within the nanotube. The kinetic inductance is nothing but a measure of the kinetic energy of the electrons. Typically for conductors as small as carbon nanotubes L_k is several orders of magnitude larger than is magnetic counterpart. In this paper we have quantified the quantum capacitance (C_q) of a variety of carbon nanotubes including different chiralities (armchair and metallic zigzag tubes) and systems of both isolated nanotubes and their bundles. The data obtained will be used to form a detailed transmission line simulation model for ULSI interconnects based on carbon nanotube technology.

This rest of this paper is organized as follows. Section 2 describes the concept of quantum capacitance and how they will be evaluated for the carbon nanotube systems under consideration. In Sect. 3, we describe the methodology employed in obtaining first-principles data. Finally in Sect. 4, we discuss the results obtained from our calculations and provide a discussion in context of VLSI interconnections.

Quantum Capacitance

Consider a capacitor connected to a battery with a bias V_a applied across it. Let us assume that both plates have a chemical potential μ_0 and are in thermal equilibrium as shown in Fig. 1a. The application of this bias causes the conduction bands in the left and right plates to shift by amounts $q\Delta V_1$ and $q\Delta V_2$, respectively, as shown in Fig. 1b. The shift in bands does not introduce any new charges, and bulk of the capacitor plates is electrically neutral. However, the coupling between the plates causes charges to move from one plate to the other in accordance with standard electrostatics. The amount of charge developed is related to the applied bias through its geometrical capacitance C_{es}. In a macroscopic system, the plates are assumed to have infinite density of states and the small redistribution of charge between the plates does not cause any perceivable change in the chemical potential in the capacitor plates.

This is, however, not true for a mesoscopic capacitor, where the density of states is usually small. The redistribution of even a small amount of charge between the plates causes a significant change in the Fermi levels in the plates. As a result, we see that the potential in the plates deviates from its equilibrium value by an amount $\Delta\mu_i$ where the index $i = (1, 2)$ represents the left and the right plate, respectively, as shown in Fig. 1c. The amount of charge developed on plate i is then given by

$$\Delta Q_i = q n_i(E)(\Delta\mu_i - q\Delta V_i) \tag{1}$$

where $n_i(E)$ represents the density of states in plate i. It may be noted that $\Delta Q_1 = \Delta Q_2$ since the charge removed from one plate is put on the other plate. Using (1) and the fact that $\Delta V_a = \Delta V_1 + \Delta V_2$ we can find the experimentally observed electrochemical capacitance [5] defined by $C_\mu \equiv q\Delta Q/\Delta\mu$ where

$$\frac{1}{C_\mu} = \frac{1}{C_{es}} + \frac{1}{C_q} \tag{2}$$

where C_{es} is the electrostatic capacitance defined by $C_{es} = \Delta Q/\Delta V_a$ and the quantum capacitance C_q given by

$$\frac{1}{C_q} = \frac{1}{q^2}\left(\frac{1}{n_1(E)} + \frac{1}{n_2(E)}\right) \tag{3}$$

The concept of quantum capacitance was first suggested by Luryi [6] to explain finite size quantization effects observed in a 2D electron gas (2DEG). Typically the process of adding an extra electron to a conducting channel above the Fermi level involves the expenditure of an insignificant amount of energy. However, in mesoscopic systems like a 2DEG or a carbon nanotube, the effects of quantization of energy states similar to the appearance of discrete states in a 1D quantum well problem results in a non-zero expenditure of energy when a particle is added to

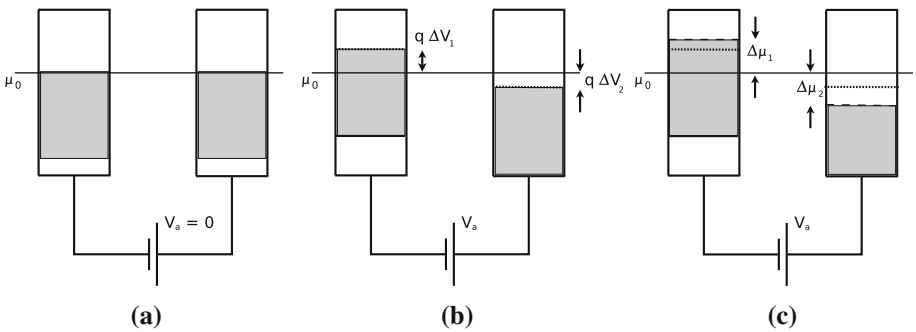

Fig. 1 Energetics of a capacitive element. **a** The conduction bands (shown by the *shaded region*) under equilibrium, **b** In a macroscopic capacitor on application of a bias, the bands shift by an amount $q\Delta V_i$, where $i = 1, 2$ represent the *left* and *right* plates, respectively. **c** In a mesoscopic capacitor, the charge redistribution due to coulombic coupling causes the bulk to lose its charge neutrality. The chemical potential changes by an amount $\Delta\mu_i$ from its equilibrium value μ_0

the lowest vacant state above the Fermi sea of electrons. Hence, not surprisingly quantum capacitance appears in the RF circuit model derived by authors in [4]. We can extract this parameter easily from the bandstructure information that we have generated though first-principles calculations. If we ignore electrostatic interaction, [7] i.e., there is no charge redistribution due to coulomb coupling, the effective capacitance is given by

$$C = C_q = q\frac{\partial Q}{\partial \mu} = \frac{\partial Q}{\partial V_a} \tag{4}$$

The free charge density in a semiconductor can be written as

$$Q = q\int_0^{+\infty} n(E)\left(f\left(E+\frac{E_g}{2}+qV_a\right)-f\left(E+\frac{E_g}{2}-qV_a\right)\right)dE \tag{5}$$

where $n(E)$ is the density of states, V_a is the applied voltage and $f(E)$ is the Fermi–Dirac distribution. The Fermi level E_f is assumed to be mid gap when $V_a = 0$. To generalize this for metals, we just set the energy gap $E_g = 0$. For this study we are only interested in low lying excitations in the first (metallic) sub-band limiting our integration in (5) before the first Van Hove singularity is encountered in the 1D density of states (approximately the order of 1 eV around E_f) . Since the density of states encountered in the single walled nanotube is a constant in this range, due to the linear Energy-wavevector relationship, (which is incidentally core to the TL model) the value of C_q is independent of applied bias and is given by

$$C_q = \frac{2\eta q^2}{h v_f} \tag{6}$$

where the Fermi velocity is given by $v_f = \hbar^{-1}\partial E/\partial k$ and η is the number of bands contributing at a given energy. The band structure of single-walled metallic carbon nanotubes exhibit linear energy-wave vector dispersion in the vicinity of the Fermi level. Hence, it becomes convenient to compute quantum capacitance using (6), since $\partial E/\partial k$ is a constant. When considering more complex systems like carbon nanotube bundles, this is no longer true and the Fermi velocity becomes energy dependent. It is much convenient to extract the quantum capacitance using Eqs. (4) and (5). The quantum capacitance calculations for the nanotubes bundles are at $E = E_f$.

Computational Methodology

The calculations presented in this paper are strongly dependant on the electronic structure, the nanotube systems under consideration. The bandstructure was calculated through ab-initio computations calculated using the plane wave codes implemented in PWscf 3.2 distribution [8] on a 2.8 GHz Intel Core 2 CPU based machine with 1GB of physical memory.

This section describes a brief account of the employed methodology and the simulation parameters used in our work. The electronic structure calculations were preceded with an optimization of the carbon nanotube unit cell geometries. First, the approximate coordinates of the carbon atoms in the nanotube unit cell were calculated using simple formulae available in published literature [9]. The unit cells were then subjected to a Broyden-Fletcher-Goldfarb-Shanno (BFGS) nonlinear optimization procedure and relaxed to their most stable geometry. The optimization procedure essentially involved varying the unit cell dimensions in such a way so as to find a minimum of the total energy, which was calculated self-consistently. To ensure that the supercell of the individual tube used was big enough to ignore intercell interaction, the relaxation runs were performed with a hexagonal and a cubic lattice similar to the methodology employed in [10].

Calculations pertinent to SWNT bundles require that an equilibrium intertube spacing be found in order to capture quantum coupling effects properly. This was done by first relaxing all the individual unit cells using the method described earlier. We use the relaxed unit cell and adjust the lattice parameter such that total energy of the system is minimized. SWNT lattices are experimentally known to be hexagonal hence only such lattice geometries were considered for them. Our calculations used the Von Barth-Car ultrasoft pseudopotentials (USPP) [11] with Perdew Zunger [12] exchange and correlation (local density approximation (LDA) paradigm). The use of USPPs reduces the overall computation workload significantly, and we were able to obtain numerical convergence with a relatively small energy cutoff when compared to those required by norm conserving pseudopotentials (NCPPs). The simulation parameters for the relaxation runs are tabulated below (see Table 1). A small Gaussian smearing was also applied to ensure that the integration of the SCF energy over the Brillouin zone converged. This is necessary as the systems are expected to be metallic. SCF Convergence threshold was set to 1×10^{-6} Ry. Brillouin zone integration for the relaxation runs was carried out on a $4 \times 4 \times 4$ k-point Monkhorst pack (MP) grid [13] comprised of 32 k-points

Table 1 Simulation parameters used in relaxation calculations

Pseudopotential	Von Barth Car USPP-PZ
Kinetic energy cutoff	40 Ry.
Charge density cutoff	160 Ry.
Charge mixing β	0.3
Smearing	Gaussian (0.02 Ry.)

within the first Brillouin zone taking into account symmetry operations. All the nanotube bundles considered in this study relaxed to a mean intertube separation of 3.2 Å.

Our studies have included a variety of nanotube systems with diameters ranging from 5 to 12 nm. We have performed calculations for single walled tubes and bundles that constitute of these individual tubes. The calculations for SCF were done with a denser K-point mesh compared to that used for the structural relaxation runs. For the nanotube bundles, an 8 × 8 × 8 MP grid and a 50–80 Ry. kinetic energy cutoff was found sufficient for numerical convergence of total energy. Other than that, all other simulation parameters were similar to that in Table 1. Band structure calculations for the single walled tubes were performed using 20 linearly spaced k-points along the z-direction of the tube i.e. $0 \leq \vec{k}_z < \pi/a_0$ for armchair tubes and $0 \leq \vec{k}_z < \pi/\sqrt{3}a_0$ for zigzag tubes, for armchair tubes and for zigzag tubes, where $a_0 = 2.47$ Å is the lattice constant of Graphene.

Results and Discussion

Single Walled Carbon Nanotubes

In this section we pay attention to results drawn for an isolated single walled carbon nanotube. Quantum capacitance results are presented for four armchair and three zigzag tubes in Table 2. The diameter of these tubes ranging from 5 to 12 nm. The results were all derived from dispersion relations calculated using the methodology described in the previous section. In general, there is a very weak variation of C_q with respect to chirality of the tube. Zigzag tubes exhibited much higher quantum capacitance compared to the armchair varieties. The reason for this can be explained on the basis of the number of states contributing at the Dirac point. An armchair (m, m) tube has two sub-bands crossing the Fermi energy E_f at $\vec{k}_z = 2\pi/3a$ (Fig. 2a) within the irreducible Brillouin zone. Hence, we take $\eta = 2$ when calculating C_q. For zigzag (m, 0) tubes, we take $\eta = 4$ since the conduction and valence bands cross-meet (Fig. 2b) at $\vec{k}_z = 0$ and each of these bands are doubly degenerate. The C_q values are presented for the metallic conduction sub-band only where the density of states (and hence C_q) is a constant for all single walled nanotubes. This is a good assumption because the first Van Hove singularity in the electronic density of states occurs at about 0.7 eV away from the Fermi level for all tubes, which is essentially the limits of the voltages we are interested in operating the nanowires for most electronic applications. Table 2 also includes values for the Luttinger interaction parameter 'g' calculated for the individual tubes in a microstrip configuration. The tube is assumed to be immersed in a lossless dielectric of $\varepsilon_r = 3.9$, 50 nm above a perfectly conducting ground plane. The parameter g can be calculated as

$$g = \left(1 + \frac{2\eta C_q}{C_{es}}\right)^{-1/2} \tag{7}$$

Here, C_{es} is the electrostatic capacitance of the system under consideration. These numbers for the electrostatic capacitance were drawn from our previous research work on electrostatic capacitance extraction for different nanotube interconnect configurations [14]. We get g to range between 0.14 and 0.33. Both zigzag tubes show a similar 'g' values that were considerably smaller (g = 0.14) than those for the armchair varieties. Readers must note that 'g' values were calculated by linearizing the dispersion curves near the Fermi levels. The linearizing around the Fermi level is especially important for the smaller (4,4), (5,5) tubes in the system for which our calculations show small band gaps opening up as the result of tube curvature. Our results compare well with experiments reported by authors in [15, 16, 17, 18]. An experiment by [18], however, suggests a much smaller observed quantum capacitance value for one of their metallic specimens. It may be of interest to note that 'g' values indicate faster plasmon propagation speeds. The propagation velocity is related to 'g' as $v_p = v_f/g$. To compare with copper ($v_f \approx 1.57 \times 10^6$ m/s) a (12,0) tube is predicted to have a plasmon velocity $v_p \approx 6.02 \times 10^6$ m/s. This is what would make SWNT-based interconnects extremely competitive as interconnects for nanoscale integrated circuits.

Table 2 Quantum capacitances for metallic SWNTs

Type	C_q (fF/μm)	Luttinger interaction parameter 'g'
(4,4)	0.214	0.27
(5,5)	0.221	0.25
(8,8)	0.14	0.33
(9,9)	0.207	0.28
(9,0)	0.388	0.14
(12,0)	0.366	0.14

Bundled Carbon Nanotubes

Clustering of the carbon nanotubes into crystalline ropes induces further changes in the electronic dispersion along the tube axis. The bundles we have considered in this paper are perfect crystalline nanotube bundles, which are comprised of identical single walled nanotube constituents with an intertube separation of 3.2 Å. The most prominent

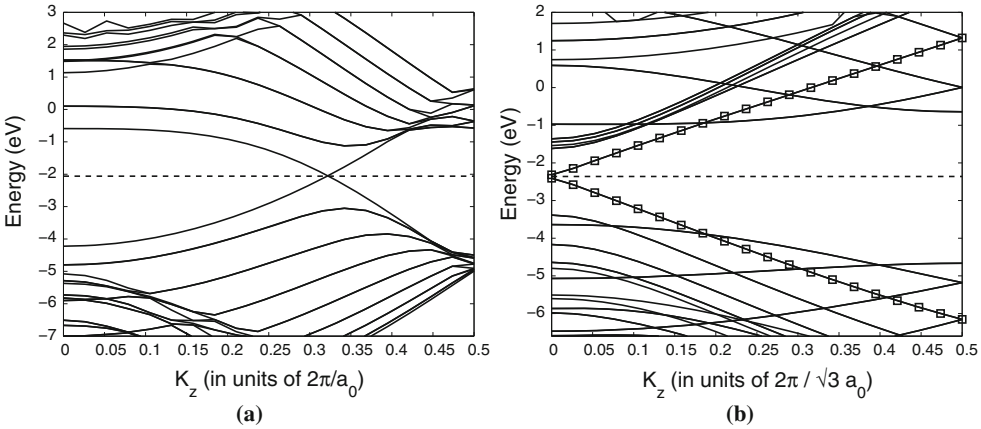

Fig. 2 One-dimensional bandstructure for **a** (8,8) armchair carbon nanotube along the z direction, with $0 < k_z < \pi/a_0$ and a **b** (12,0) zigzag nanotube with $0 < k_z < \pi/\sqrt{3}a_0$ where $a_0 = 2.47$ Å is the lattice constant of Graphene. The Fermi levels for the armchair and zigzag tubes are at -2.06 and -2.36 eV, respectively, shown by the dotted lines. The marker on **b** indicates degenerate bands

feature from the point of view of quantum capacitance is that the number of states at the Fermi level is significantly enhanced and is no longer a constant. The simple Eq. (6) cannot be used to approximate C_q since the density of states at the Fermi level is no longer a constant. Our calculations show that there is a significant increase in the density of states around E_f. This results in a much larger in magnitude compared to single walled tubes. Using the density of states information, we can approximate quantum capacitance as

$$C_q = q^2 N(E_f) \tag{8}$$

where $N(E)$ is the density of states at an energy E. The results for SWNT bundles are presented in Table 3, which illustrate the dependence of quantum capacitance on individual tube chirality and the computed equilibrium spacing between the tubes. SWNT bundles exhibit much larger quantum capacitance per tube when compared to their constituent nanotubes. To make the comparison with individual tubes, we calculate a parameter C'_q, which is nothing but the individual contribution of each tube within a bundle. This number is nothing but the quantum capacitance of the unit cell divided by the mean volume occupied by each constituent nanotube within the bundle. As we can see the coupling effect is quite pronounced and results in a much higher density of states at the Fermi level when compared to that of an individual nanotube. This effect is illustrated in Fig. 3, which compares the electronic density of states of a (5,5) nanotube bundle with its constituent

Table 3 Quantum capacitance for crystalline SWNT bundles

Type	Intertube spacing (Å)	C_q (nFμm^{-3})	C'_q (fF $tube^{-1}\mu m^{-1}$)
(4,4)	3.15	1.228	15.51
(5,5)	3.2	1.175	17.2
(8,8)	3.1	0.569	11.16
(9,9)	3.05	0.376	8.34
(9,0)	3.18	0.819	16.02

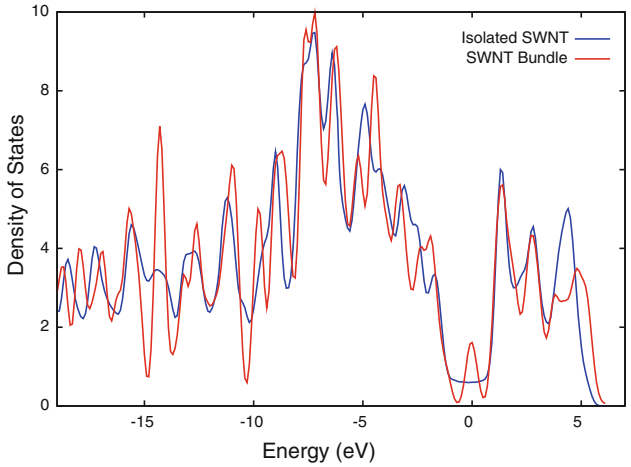

Fig. 3 Density of states comparison of a (5,5) isolated SWNT vs. a (5,5) SWNT bundle. Note the enhanced density of states at the Fermi level. The Fermi levels of both plots are centered on 0 eV. This increased density of states will yield a higher quantum capacitance per unit volume for a bundle when compared to its constituent individual tube

tubes obtained through a plane wave calculation. The Fermi levels for both systems have been aligned at $E = 0$. As mentioned earlier, the density of states in a bundle within the first sub-band is not a constant unlike an isolated SWNT.

To identify the source of this enhanced quantum capacitance, we project the density of states information onto the s and p orbitals at each lattice site within the unit cell (see Fig. 4). The local contributions were all summed up to yield total contributions from each valence orbital. It was found that all the extra contribution to the state enhancement came out through intertube interactions between the p_x and p_y orbitals, both of which are out of the plane of the nanotube's surface (circumference in the $x-y$ plane). This corresponds to intertube interactions between the unhybridized p_z orbitals within the Graphene sheet model of the nanotube. These interactions manifest as energy states localized in the intertube spacing within the

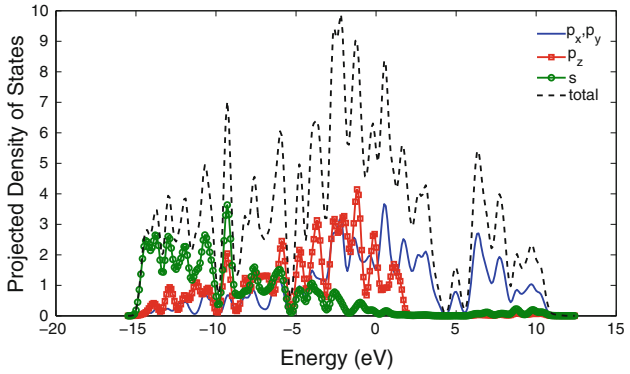

Fig. 4 Projected density of states of the (5,5) SWNT bundle over atomic orbitals as well as the total density of states

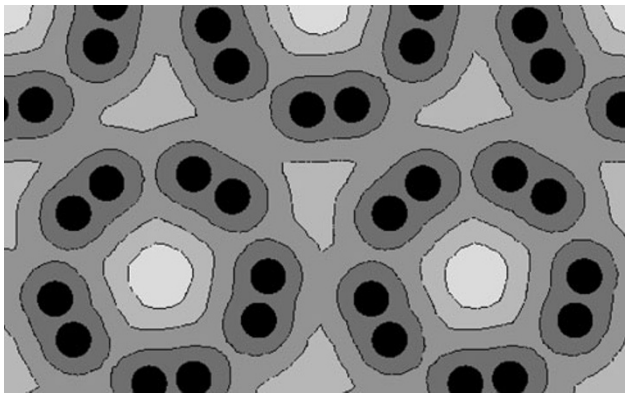

Fig. 5 Local density of states of a (5,5) SWNT bundle near the Fermi level. The interaction between neighboring tubes is clearly visible. *Dark spots* indicate position of carbon atoms

bundle (Fig. 5). The contour plot is a visualization of local density of states (LDOS) in the vicinity of the Fermi Level in a (5,5) SWNT bundle along the circumferential plane of the bundle.

Conclusions

In this paper, we have characterized individual metallic carbon nanotubes and crystalline nanotube bundles for their quantum capacitance, to model the high-frequency transmission line interconnects comprised of these nanotubes. We have seen that the quantum capacitance of individual tubes have a very weak dependence on chirality. Zigzag tubes owing to the presence of degenerate bands around the Fermi level exhibit almost twice the quantum capacitance compared to the armchair varieties. The value of the Luttinger parameter 'g' was estimated between 0.14 and 0.33.

The zigzag varieties exhibit a much smaller interaction parameter ($g = 0.14$). Consequently, they have an advantage over armchair tubes and even bulk Copper in terms of signal propagation delay. When put in a bundle, the electronic density of states shows a significant increase around the Fermi level, due to electronic coupling between 2p orbitals oriented normal to the tube surface, thus markedly increasing the value of C_q per unit cell when compared to the constituent nanotube. Bundled nanotubes also show a poor C_q dependence on the chirality of its constituent tubes.

Acknowledgements and Disclaimer The research reported in this document was performed in connection with contract DAAD17-03-C-0115 with the US Army Research Laboratory. The views and conclusions contained in this document are those of the authors and should not be interpreted as presenting the official policies or position, either expressed or implied, of the US Army Research Laboratory or the US Government unless so designated by other authorized documents. Citation of manufacturer's or trade name does not constitute an official endorsement or approval of the use thereof. The US Government is authorized to reproduce and distribute reprints for Government purposes notwithstanding any copyright notation hereon.

References

1. International technology roadmap for semiconductors, interconnect (2005)
2. F.D.M. Haldane. Luttinger liquid theory of one-dimensional quantum fluids. i. properties of the luttinger model and their extension to the general 1d interacting spinless fermi gas. J. Phys. C: Solid State Phys. **14**(19), 2585–2609 (1981)
3. M. Bockrath, *Carbon nanotubes: electrons in one dimension*. PhD thesis, UC Berkeley (1999)
4. P. Burke Luttinger liquid theory as a model of the gigahertz electrical properties of carbon nanotubes. Nanotechnol., IEEE Trans. **1**, 129–144 (2002)
5. M. Büttiker, H. Thomas, A. Pretre. Mesoscopic capacitors. Phys. Lett. A **180**, 364–369 (1993)
6. S. Luryi. Quantum capacitance devices. Appl. Phys. Lett. **52**(6), 501–503 (1988)
7. D.L. John, L.C. Castro, D.L. Pulfrey. Quantum capacitance in nanoscale device modeling. J. Appl. Phys. **96**(9), 5180–5184 (2004)
8. P. Giannozzi. http://www.quantum-espresso.org
9. R. Saito, G. Dresselhaus, M.S. Dresselhaus, *Physical properties of carbon nanotubes*. World Scientific Publishing Company, September 1998
10. J. Kürti, G. Kresse, H. Kuzmany. First-principles calculations of the radial breathing mode of single-wall carbon nanotubes. Phys. Rev. B **58**, R8869–R8872 (1998)
11. We used the pseudopotential c.pz-vbc.upf from http://www.quantum-espresso.orgdistribution
12. J.P. Perdew, A. Zunger. Self-interaction correction to density-functional approximations for many-electron systems. Phys. Rev. B **23**, 5048–5079 (1981)
13. H.J. Monkhorst, J.D. Pack. Special points for brillouin-zone integrations. Phys. Rev. B **13**, 5188–5192 (1976)
14. V. Parkash, A. Goel. Electrostatic capacitance extraction for carbon nanotube interconnects. in *Circuits and Systems, 2008.*

MWSCAS 2008. 51st Midwest Symposium on, pp. 834–837, Aug. 2008.
15. M. Bockrath, D.H. Cobden, A.G. Rinzler, R.E. Smalley. Luttinger-liquid behavior in carbon nanotubes. Nature **397** 598, (1998)
16. S. Ilani, L.A.K. Donev, M. Kindermann, P.L. McEuen. Measurement of the quantum capacitance of interacting electrons in carbon nanotubes. Nat. Phys. **2**, 687–691 (2006)
17. H. Ishii, H. Kataura, H. Shiozawa, H. Yoshioka, H. Otsubo, Y. Takayama, T. Miyahara, S. Suzuki, Y. Achiba, M. Nakatake, T. Narimura, M. Higashiguchi, K. Shimada, H. Namatame, M. Taniguchi. Direct observation of tomonaga-luttinger-liquid state in carbon nanotubes at low temperatures. Nature **426**(6966), 540–544 (2003)
18. J. Dai, J. Li, H. Zeng, X. Cui. Measurements on quantum capacitance of individual single-walled carbon nanotubes. Appl. Phys. Lett. **94**, 093114 (2009)